SSSH 54
ISSN 0140 3818

UNIVERSITY OF SOUTHAMPTON

DEPARTMENT OF SHIP SCIENCE

FACULTY OF ENGINEERING AND APPLIED SCIENCE

THE PREDICTION OF RUDDER-PROPELLER INTERACTIONS USING BLADE ELEMENT-MOMENTUM THEORY AND MODIFIED LIFTING LINE THEORY

by A.F. Molland

Ship Science Report No. 54

January 1992

SSSU 54
ISSN 0140 3818

UNIVERSITY OF SOUTHAMPTON

DEPARTMENT OF SHIP SCIENCE

FACULTY OF ENGINEERING AND APPLIED SCIENCE

THE PREDICTION OF RUDDER-PROPELLER INTERACTIONS USING BLADE ELEMENT-MOMENTUM THEORY AND MODIFIED LIFTING LINE THEORY

by A.F. Molland

Ship Science Report No. 54

January 1992

THE PREDICTION OF RUDDER-PROPELLER INTERACTIONS USING BLADE ELEMENT-MOMENTUM PROPELLER THEORY AND MODIFIED RUDDER LIFTING LINE THEORY

by

A.F. Molland

Ship Science Report No. 54

University of Southampton

January 1992

1. INTRODUCTION

Extensive experimental results of tests to determine the influence of propeller loading on ship rudder performance are reported in Refs. 1 and 2. Complimentary theories have been developed to provide some theoretical evidence for the form of the experimental data, and to allow an extension of the experimental results. These theories have entailed the use of a full lifting surface approach, Ref. 3., and a simpler approach using lifting line theory, the development of which is the subject of this report.

In the theoretical analysis, lifting line theory, modified to include the specific features of the low aspect ratio rudder, the influence of the propeller upstream, and to account for the differences between theory and experiment, is used to predict the spanwise load distributions.

An outline of the theoretical analysis is given, together with some comparisons with experimental data. Examples are presented of a parametric study which uses the theory to investigate variations in rudder and propeller particulars.

2. GENERAL DESCRIPTION OF THE THEORETICAL MODEL

2.1 The basic rudder-propeller layout is shown in Fig. 1. The rudder is modelled as a lifting line with suitable spanwise input velocity and incidence distributions which result from propeller action upstream.

The propeller is modelled using blade element/momentum theory. This basically provides a means of estimating the induced axial and circumferential velocities at the propeller blades.

The basic propeller theory requires additional features to take account of the behaviour of the fluid between the propeller and the rudder, the influence of adjacent hull on the propeller and the influence of the rudder on the propeller. These various features are summarised in the following sections.

2.2 The basic theory produces the induced velocities at the propeller blades. An averaging factor is required to produce the circumferential mean value at each propeller radius.

2.3 Following the behaviour of the fluid upstream of the propeller there is a further acceleration and contraction of the propeller slipstream between the propeller disc and the rudder, Fig. 2(a).

2.4 Blockage effects between the propeller and adjacent hull (or wind tunnel groundboard) result in a backflow and an effective reduction in axial velocity over that adjacent part of the rudder, Fig. 2(b).

2.5 Blockage effects due to the rudder lead to a reduction in velocity over the propeller (as a whole), Fig. 2(c).

2.6 Upwash ahead of the rudder when at incidence leads to an induced crossflow in way of the propeller disc, Fig. 2(d).

2.7 At zero incidence the induced velocities at the rudder may be derived from a vertical cut through the slipstream on the propeller centreline. If the rudder stock is not at the leading edge then at positive or negative rudder incidence the cut will be taken some distance off the propeller centreline, Fig. 2(e); with a finite rudder thickness the effective velocity vectors at the cut will differ between the top and bottom of the slipstream, the direction of the asymmetry being inverted for change from positive to negative rudder incidence. A similar effect exists if the centreline of the rudder does not coincide with the centreline of the propeller.

3. PROPELLER THEORY

3.1 Basic Theory

The propeller induced velocities are derived using an adaptation of blade-element-momentum (BEM) theory. This theory is described in some detail in Refs 4 and 5 and a successful working version of the approach is described in Ref. 6. A summary of the equations derived from the theory and employed in the current analysis is given in Appendix 1.

Axial and rotational velocity inflow factors, and hence induced axial and rotational velocities, are derived from momentum theory together with the use of Goldstein correction factors to take account of a finite number of blades.

Section thrust and torque is modelled using blade element theory in which the propeller blade is divided into a number of elemental sections. Local section lift and drag characteristics are obtained using relevant lift and drag coefficients for the particular local section type, thickness and chord length. Sources used for the derivation of such section data include Refs. 5 and 7.

Combination of the momentum and blade element theories yields a solution for the local

thrust (dT), torque (dQ) and efficiency at each elemental section. Integration of the section thrusts and torques radially across the blade yields the total thrust, torque and efficiency for each blade and hence for the propeller.

3.2 Comparison of Basic Propeller Theory with Experimental Results:

Fig. 3 illustrates the theoretical estimates of K_T and K_Q compared with the experimental values for the Wageningen B4.40 propeller.

It is seen that the theoretical predictions are similar to the experimental results over much of the propeller working range.

A basic asssumption in the current analysis is that the distributions of dK_T/dx and dK_Q/dx are also broadly corrrect leading to realistic distributions of the axial (a) and circumferential (a') inflow factors. Examples of basic distributions of V(1+a) and propeller induced flow angle β at the propeller are shown in Fig. 4.

3.3 Additions/Modifications to the Basic Theory

3.3.1 Circumferential mean velocities:

Goldstein K factors are applied also to the downstream induced velocities (a and a') to yield the mean induced velocity and angle at each radius. The influence of this application (at J = 0.35) is shown in Fig. 4.

3.3.2 Slipstream acceleration:

A Gutsche type correction, Ref. 8, is applied to a and a' to account for the fluid acceleration between the propeller and rudder. This amounts to a simple correction based on the distance of the rudder from the propeller (X/D), Fig. 1, and can be represented as:

$$K_R = 1 + 1/(1+0.15/(X/D))$$

whereby the induced axial and circumferential inflow factors become $K_R.a$ and K_Ra' and the axial and tangential velocities become:

$$V_{AR} = V(1+K_R.a)$$
$$V_{TR} = K_R.a'\Omega r$$

Examples of the use of this correction (for J = 0.35) are shown in Fig. 5

3.3.3 Slipstream contraction:

Slipstream contraction is estimated by applying continuity between the propeller and rudder and using, as a first approximation, the axial velocity changes derived by the Gutsche correction. This results in a slipstream diameter at the rudder (D_R) relative to the propeller disc diameter (D) as follows:

$$D_R/D = [(1+a)/(1+K_R.a)]^{1/2}$$

3.3.4 Propeller inflow velocity reduction due to rudder blockage effects:

Approximate values of this velocity reduction were derived from experimental data, Refs 1 and 9. Namely, the presence of the rudder at given propeller revs causes an increase in K_T which can be interpreted as an effective decrease in J (or velocity).

Values derived from the experimental data, assumed constant across the J range, are tabulated as follows:

X/D	Mean $+\Delta K_T$	Approx $-\Delta J$
0.30	0.025	0.075
0.39	0.025	0.075
0.52	0.015	0.045

Thus, in the theoretical model, the rudder blockage is incorporated in the analysis as an effective decrease in J.

3.3.5 Tangential induced velocity at the propeller disc due to rudder upwash:

The complimentary lifting surface work reported in Ref. 3 was used to provide guidance on likely rudder upwash values at the propeller. Variation of these values across the rudder, for changes in rudder angle are shown in Fig. 6. Average values are shown in Fig. 7.

In the current analysis the average upwash angle (ϵ) for a given rudder angle (δ) has been applied as a constant value across the propeller. This leads to a modification to the circumferential inflow as follows:

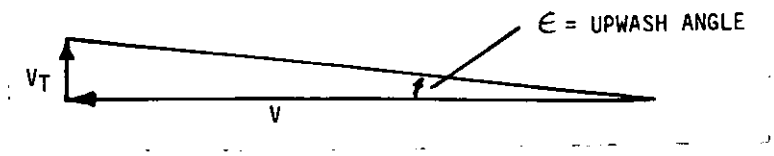

$$V_T/V = \tan \epsilon$$

$$V_T/V = 2\pi nra''/V \quad \text{(where } a'' \text{ = race rotation factor due to tangential flow)}$$

$$= \pi x \frac{nD}{V} . a'' = \frac{\pi x}{J} a''$$

$$\text{or} \quad a'' = \frac{V_T}{V} \cdot \frac{J}{\pi x} = \frac{V_T}{V} . \tan \psi$$

a" is then applied to the blade element vector diagram (in a positive sense over one half of the propeller and a negative sense over the other half) as follows:

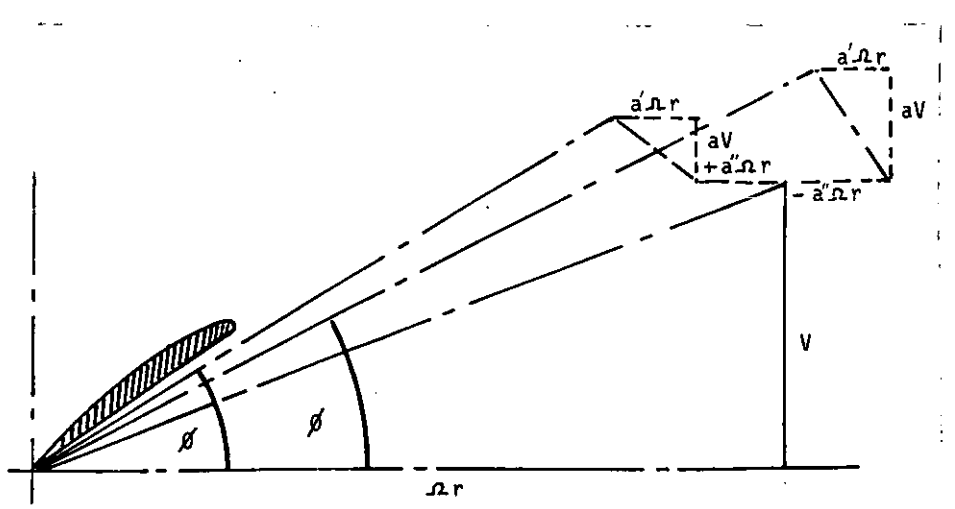

This leads to amendments to the basic equations (Appendix 1) as follows:

$$a = \frac{1 - \eta_i \pm a''}{\eta_i + \frac{\tan^2\psi}{\eta}} \qquad \text{modified Eqtn. (A9)}$$

$$a' = 1 - \eta_i(1+a) \pm a'' \qquad \text{modified Eqtn. (A8)}$$

$$\text{and} \quad \frac{dK_T}{dx} = \frac{\pi^2}{4} \cdot \frac{Nc}{D} \cdot C_L \, x^2(1-a'\pm a'')^2 \sec\phi(1-\tan\phi\tan\gamma) \qquad \text{modified Eqtn. (A4)}$$

The ensuing modified values of a and a' are used in the subsequent downstream use/analysis of the inflow factors. An example of the influence of upwash (for $\epsilon = 8.5°$ and J = 0.51) is included in Fig. 4.

3.3.6 Blockage effects between propeller and adjacent hull:

This results in an effective reduction in induced velocity over the adjacent part of the rudder, as discussed in Section 2.4.

The theory used in the current analysis is not capable of predicting this velocity reduction. An empirical reduction factor, found by trial, is therefore applied.

3.3.7 Resolution of final fluid velocity and input angle applied to the lifting line:

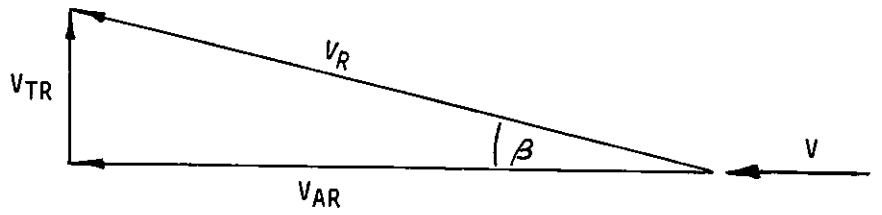

V_R = final inflow velocity

β = final inflow angle

$V_{AR} = V(1+K_R.a)$

$V_{TR} = K_R \,.\, a'\Omega r \;\; ; \;\; r = x.R \;\; ; \;\; \Omega = 2\pi n$

$$V_R^2 = V_{TR}^2 + V_{AR}^2$$

$$= 4\pi^2 n^2 r^2 (K_R.a')^2 + V^2(1+K_R.a)^2$$

$$= \pi^2 x^2 n^2 D^2 (K_R/a')^2 + V^2(1+K_R.a)^2$$

$$(V_R/V)^2 = \pi^2 x^2 \,.\, (K_R a')^2/J^2 + (1+K_R.a)^2]$$

and $$V_R/V = [\pi^2 x^2 (K_R a')^2/J^2 + (1+K_R.a)^2]^{1/2} \qquad (1)$$

$$\beta = \tan^{-1} \frac{2\pi n r K_R.a'}{V(1+K_R.a)}$$

$$= \tan^{-1} \frac{\pi x n D}{V} \cdot \frac{K_R.a'}{(1+K_R.a)}$$

$$\beta = \tan^{-1} \frac{\pi x}{J} \cdot \frac{K_R.a'}{(1+K_R.a)} \qquad (2)$$

Noting that β, as seen from the rudder, will be positive over one half of the slipstream and negative over the other half.

4. RUDDER LIFTING LINE THEORY

4.1 General:

The method used for deriving the basic spanwise load distribution is generally along the lines of that due to Glauert, Ref. 10.

Modifications for application to low aspect ratio ship rudders are made as described previously in Ref. 11. These entail incorporating downwash contributions from the tip trailing vortex and empirical corrections to take account of the differences between theoretical lift curve slopes and those derived from experiments.

Propeller induced axial and rotational velocities are modelled as local changes in lifting line input velocity, Eqtn. (1) and incidence, Eqtn. (2).

4.2 Outline of the Lifting Line Theory:

The rudder geometry used in the analysis is given in Fig. 8. The effect of the reflection plane is represented by an image rudder and vortex system. The rudder is assumed to have a total span, including its image, of 2S and a taper ratio (C_T/C_R) = T.

The rudder is considered as being replaced by a lifting line of length 2S. The coordinate y is replaced by the angle θ defined as $y = -S\cos\theta$.

At any point on the rudder, $c = C_R(1 - k\cos\theta)$ where $k = (1 - T)$ and, at any point, the incidence of the rudder, considered as a lifting line will be:

$$\bar{\alpha} = \delta \pm \beta \qquad (3)$$

where: δ = incidence of the rudder

β = fluid inflow angle at the rudder induced by the propeller

The local circulation Γ_L at a point θ on the rudder may be expressed as a Fourier series:

$$\Gamma_L = 4S\ V\ \Sigma\ An \sin n\theta \qquad (4)$$

where: V is the free-stream velocity

and since the planform is symmetrical about the mid point ($\pi/2$), only odd values of n will occur in the series.

The induced local velocity ω_L at a point θ is given by:

$$\omega_L = V(\Sigma n\ An \sin n\theta)/\sin\theta \qquad (5)$$

The section experiences a lift force corresponding to two-dimensional motion at the effective angle of incidence ($\bar{\alpha} - \omega_L/V_R$) where ω_L/V_R is the induced downwash angle. Local lift coefficient

$$C_{LL} = m(\bar{\alpha} - \omega_L/V_R) \qquad (6)$$

where m is the two-dimensional lift curve slope, allowing for thickness and viscosity effects and V_R is the local velocity at a point θ at the rudder location in way of the slipstream.

Hence at any point,

$$\Gamma_L = \frac{L_L}{\rho V_R}$$

$$= \frac{C_{LL} \cdot c \cdot V_R}{2}$$

$$= \frac{m}{2} \cdot c \cdot V_R\ (\bar{\alpha} - \omega_L/V_R) \qquad (7)$$

Incorporating the value of induced velocity from equation (5)

$$\Gamma_L = \frac{m}{2} \cdot c \cdot V_R\ (\bar{\alpha} - \frac{V}{V_R}\ (\Sigma\ n\ An \sin n\theta)/\sin\theta) \qquad (8)$$

equating (4) and (8) and setting $\mu = m\ C_R/8S$ leads to

$$\Sigma \left[An \sin n\theta \left(\mu n + \frac{\sin\theta}{1 - k\cos\theta} \right) \right] = \mu \cdot \bar{\alpha} \cdot \sin\theta \cdot \frac{V_R}{V} \qquad (9)$$

This fundamental equation must be satisfied at all points on the rudder between 0 and $\pi/2$.

Local lift:

$$L_L = \rho\, V_R\, \Gamma_L = \rho\, V_R\, (4SV\Sigma\, An \sin n\theta)$$

$$= 4\, \rho\, S\, V\, .\, V_R\, (\Sigma\, An \sin n\theta)$$

hence the local lift coefficient:

$$C_L = L_L / 1/2\rho\, c\, V^2$$

$$= \frac{8S}{c}\ \Sigma\, An \sin n\theta\, .\, \frac{V_R}{V}$$

$$= \frac{8S}{C_R(1 - k\, .\, \cos\theta)}\ \Sigma\, An \sin n\theta\, .\, \frac{V_R}{V} \qquad (10)$$

In this final case local lift coefficient, and its numerical integration for total lift coefficient, is based on free-stream velocity.

The fundamental equation (9) has to be satisfied at all points along the rudder. A large number of control points is desirable since the analysis has to include the facility to vary $\bar{\alpha}$ along the rudder and to superimpose a vortex at the tip. 20 control points were chosen for the current analysis.

4.3 Tip Trailing Vortex:

It is assumed, as described in Ref. 11, that the influence of the tip vortex is responsible for the non-linear component of lift normally exhibited by low aspect ratio lifting surfaces operating in a free stream. The assumption is also incorporated in the current analysis when the rudder is operating downstream of a propeller.

Based on the reasoning in Ref. 11 the equation used in the analysis for the downwash induced by the tip vortex is:

$$\alpha_T(\theta) = 0.645\, H_1(\theta)\, \alpha^2\, T^{1.5}/AR$$

where $H_1(\theta)$ is the general form of the variation of downwash across the span at a particular incidence, aspect ratio and taper ratio, and the constant is introduced to correlate the magnitude of the load with experiment at the datum angle. The distribution of $H_1(\theta)$ is shown in Fig. 9.

4.4 Correction to Theoretical Lift:

The lifting line analysis, when applied to relatively low aspect ratios, results in lift curve slopes in excess of experimentally derived values. The reasoning in Ref. 11 led to a correction to the lifting line result of the form:

$$C_{Lc} = C_{Lt} \cdot e\,(AR)$$

where: C_{Lt} is the theoretical lift from lifting line theory
C_{Lc} is the corrected lift coefficient
e is the ratio of the experimental to the theoretical and is a function of aspect ratio.

The correction proposed in Ref. 11 and adopted in the current analysis is:

$$e = 1.052\ T^{0.1} \times 0.875\ (1.14AR + 2)/(AR + 3.9)$$

5.0 ANALYSIS COMPUTER PROGRAM

The theoretical analysis, embracing the propeller theory and the rudder lifting line theory was incorporated in a computer program written in FORTRAN.

A general flow chart for the program is shown in Fig. 10. The analysis firstly derives the basic inflow factors induced by the propeller together with the necessary corrections as discussed in Section 3.3. The corrected induced velocities and angles are then interpolated at the rudder lifting line control points for use in the lifting line analysis.

For given input values of propeller J and P/D and values of rudder aspect ratio, taper, sweep and incidence, together with X/D and D/S, the program outputs the spanwise distribution of lift together with its integration for total lift.

6.0 DISCUSSION OF THE THEORETICAL RESULTS

Examples of the results of the spanwise load predictions, together with the experimental results derived from the pressure measurements (Ref. 1), are given in Figs. 11a, 11b and 11c.

The theoretical predictions are in broad agreement with the experimental results over most of the span and for most angles of attack. The area displaying the most divergence between theory and experiment is the outer part of the rudder at higher negative rudder angles of attack (-20° and -30°).

It is noted that the theory correctly predicts the return to free-stream characteristics at the tip of Rudder No. 3 (Fig. 11c).

The tip vortex is modelled reasonably well, although the values predicted by the theory for negative incidence well exceed those derived by experiment. It is possible that the propeller race is being swept further down the rudder and away from the tip at negative incidence and this possibility is receiving further attention.

The theoretical predictions for overall lift are shown in Fig. 12. Good correlation between theory and experiment is displayed which is to be expected considering the close correlation for the spanwise distributions, Fig. 11.

The theory in its current form provides an acceptable level of accuracy for design purposes. Some room for improvement exists in the applications of the corrections for rudder blockage and upwash, the influence of the hull/wall, movement of the propeller slipstream relative to the rudder with change in rudder incidence and modelling of the tip vortex. Work is continuing on the refinement of these corrections as applied to the lifting line theory.

7.0 PARAMETRIC STUDY

7.1 Parametric studies using the computer program have been carried out to provide a broad outline of the expected changes in performance with changes in propeller and rudder variables. The following describes briefly some examples of these studies.

7.2 Change in Propeller P/D for same K_T/J^2:

Results for 20° rudder incidence and three propeller pitch ratios are shown in Fig. 13a. It is seen that with increased rotational effects with increase in P/D (for same K_T/J^2) there is an increase in asymmetry of the spanwise distribution as would be expected. There is a net decrease in total lift when going from P/D of 0.75 to 1.20 of the order of 4%. These findings are broadly in agreement with those of the experimental investigation. These indicate that the governing parameter is K_T/J^2, although for detailed investigations it may be necessary to incorporate the influence of pitch ratio.

7.3 Change in Rudder Aspect Ratio:

Results for 20° rudder incidence and three aspect ratios are shown in Figs. 13b and 13c. The results follow the trends of rudder free-stream characteristics as borne out by the experimental investigation and reported in Ref. 13. It is interesting to note from Figs. 13b and 13c that the increase in lift due to increase in aspect ratio occurs mainly at the tip region where (for this investigation) the propeller induced inflow angles are in the same sense as rudder incidence and increase the net rudder angle of attack. It is noted that this will move the spanwise centre of pressure towards the rudder tip and should be borne in mind when considering detailed design.

7.4 Change in Propeller Coverage of the Rudder (D/S):

The results for 20° rudder incidence and three D/S values are shown in Fig. 13d. These results reflect those obtained experimentally and reported in Ref. 13. The results are not profound but do serve to illustrate the change in spanwise centre of pressure and total lift with change in D/S. It is however noted that these results confirm the ability of the theory to correctly model this effect.

7.5 General:

A large number of parametric studies have been carried out in the development of the theory, partly to validate the theory based on the experimental data and partly to determine the applications of the theory. The brief examples given serve to illustrate the ability of the theory to correctly model many of the design features and to provide a useful design tool.

8.0 CONCLUSIONS

8.1 The unmodified forms of the propeller and lifting line theories provide broadly correct forms of the rudder spanwise load distributions, reflecting the asymmetric loadings due to propeller induced changes in inflow velocity and angle.

8.2 The effects of the rudder on the propeller, including blockage which causes changes in effective thrust, and upwash causing increased asymmetry of the spanwise distribution, can be adequately accounted for by empirical corrections derived from experimental and lifting surface theoretical results.

8.3 Comparison with experimental results indicates that the modified theory satisfactorily models changes in the main variables such as propeller thrust loading, rudder aspect ratio and the ratio of propeller diameter/rudder span. The method does therefore provide a useful design tool for further investigation of changes in rudder and propeller geometry. Such output may

be used as design data in their own right, or incorporated in predictor equations as developed in Ref. 13.

8.4 Whilst it is accepted that lifting surface theory (e.g. Ref. 3) offers a better facility for modelling the physical conditions, the lifting line does offer a simple but effective approach to the problem with a relatively compact computer code. It can be refined using corrections from the lifting surface approach and experimental data. As such the program may be compact enough for incorporation within a manoeuvring simulation model. This is considered to be an attractive proposition and work is continuing along these lines.

8.5 Further developments in hand to improve the lifting line model include the facility to output spanwise centre of pressure, to estimate induced drag (along the lines adopted in Ref. 11) and to further refine the empirical corrections such as rudder induced cross flow on the propeller.

ACKNOWLEDGEMENTS

The work described in this report covers part of a research project funded by the SERC/MOD through the Marine Technology Directorate Ltd. under research grant Ref. No GR/E/65289.

NOMENCLATURE

a) Propeller:

a	:	Axial inflow factor
a'	:	Circumferential inflow factor
a"	:	Tangential inflow factor
c	:	Blade element chord
C_D	:	Drag coefficient
C_L	:	Lift coefficient
C_{L_i}	:	Ideal lift coefficient
D	:	Propeller diameter
D_R	:	Slipstream diameter at the rudder
dT	:	Thrust on local element
dQ	:	Torque on local element
J	:	Propeller advance coefficient (V/nD)
K	:	Goldstein correction factor
K_R	:	Gutsche slipstream acceleration factor

K_T : Thrust coefficient ($T/\rho n^2D^4$)

K_Q : Torque coeffcient ($Q/\rho n^2D^5$)

n : Propeller revs/sec

N : Number of blades

P : Pitch

Q : Propeller torque

r : Radius of elemental section

R : propeller radius

t : Thickness of blade element

T : Propeller thrust

U : Relative inflow speed to propeller section

V : Propeller speed of advance (or free-stream velocity)

V_T : Tangential velocity at propeller induced by rudder

x : Non-dimensional coordinate (x = r/R)

α : Section angle of attack (relative to inflow direction)

α_i : Section ideal angle of attack

γ : Defined as $\tan^{-1}(C_D/C_L)$

ϕ : Hydrodynamic pitch angle

ψ : Defined as $\tan^{-1}(J/\pi x)$

Ω : Propeller angular velocity, rads/sec (= 2πn rps)

ρ : Density of water

b) Rudder:

A : Total rudder area

AR : Effective aspect ratio

A_n : Coefficients in Fourier series for spanwise load distribution

c : Chord

$\bar{c}$: Mean chord $(C_T+C_R)/2$)

C_T : Tip chord

C_R : Root chord

C_L : Lift coefficient ($L/1/2\rho AV^2$)

e : Lift curve slope experimental correction factor

$H_1(\theta)$: General form of downwash variation induced by tip vortex

k : Defined as (1-T) in lifting line analysis

L : Lift force normal to flow direction

m : Two-dimensional lift curve slope

S : Rudder span

T	:	Taper ratio (C_T/C_R)
X	:	Distance of rudder from propeller (Fig. 1)
y	:	Spanwise coordinate in lifting line analysis
V_R	:	Fluid flow velocity at rudder
$\bar{\alpha}$	:	Effective rudder incidence ($\delta \pm \beta$)
β	:	Final propeller induced flow input angle at rudder
δ	:	Rudder incidence
ϵ	:	Rudder upwash angle (at propeller location)
Γ	:	Circulation
θ	:	Spanwise coordinate in lifting line analysis
μ	:	Coefficient in lifting line analysis
ω	:	Induced normal velocity

REFERENCES

1. Molland, A.F. and Turnock, S.R. 'Wind Tunnel Investigation of the Influence of Propeller Loading on Ship Rudder Performance'. University of Southampton, Ship Science Report No. 46, 1991.

2. Molland, A.F. and Turnock, S.R. 'Further Wind Tunnel Tests on the Influence of Propeller Loading on Ship Rudder Performance'. University of Southampton, Ship Science Report No. 52, 1992.

3. Turnock, S.R. 'Lifting Surface Method for Modelling Ship Rudders and Propellers'. University of Southampton, Ship Science Report No. 50, 1992.

4. Eckhard, M.K. and Morgan, W.B. 'A Propeller Design Method'. Transactions of the Society of Naval Architects and Marine Engineers in America (SNAME), Vol. 63, 1955.

5. O'Brien, T.P. 'The Design of Marine Screw Propellers'. Hutchingson, London, 1962.

6. Tang, A. 'Propeller Performance Estimates using Blade Element-Momentum theory'. University of Southampton, B.Sc. Honours Report No. SS204, 1985.

7. Abbot, I.H. and Von Doenhoff, A.E. 'Theory of Wing Sections'. Dover Publications, New York.

8. Gutsche, F. 'Die Induktion der Axialen Strahlzusatzgeschwindigheit in der Umgebung der

Schraubenebene'. Schiffstecknik, Heft 12/13, 1955.

9. Stierman, E.J. 'The Influence of the Rudder on the Propulsive Performance of Ships - Part I'. International Shipbuilding Progress, 36, No. 407, 1989.

10. Glauert, H. 'The Elements of Aerofoil and Airscrew Theory'. Cambridge University Press.

11. Molland, A.F. 'A Method for Determining the Free-Stream Characteristics of Ship Skeg-Rudders'. International Shipbuilding Progress, Vol. 32, No. 370, 1985.

12. Molland, A.F. and Turnock, S.R. 'Wind Tunnel Test Results for a Model Ship Propeller Based on a Modified Wageningen B4.40'. University of Southampton, Ship Science Report No. 43, December 1990.

13. Molland, A.F. and Turnock, S.R. 'The Prediction of Ship Rudder Performance Characteristics in the Presence of a Propeller'. Proc. of Conference, Manoeuvring and Control of Marine Craft 92, MCMC92, University of Southampton, 1992.

APPENDIX 1

SUMMARY OF EQUATIONS DERIVED FROM BLADE-ELEMENT MOMENTUM THEORY:

a) Momentum Considerations:

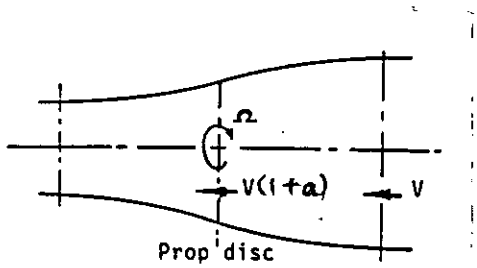

Velocity at disc = V(1 + a)

Angular velocity relative to blades at disc = $\Omega(1 - a')$

where V = speed of advance of propeller

Ω = angular velocity of propeller

a = axial inflow factor

a' = circumferential inflow factor

Equating the thrust on an element of the blade to the axial momentum change, the torque on an element to the angular momentum change and introducing a Goldstein K factor to take account of a finite number of blades, leads to the following equations for the thrust and torque gradients:

$$\frac{dK_T}{dx} = \pi J^2 \, xKa(1+a) \qquad (A1)$$

$$\frac{dK_Q}{dx} = \frac{\pi^2}{2} \, . \, J \, . \, x^3 Ka'(1+a) \qquad (A2)$$

and for local efficiency:

$$\eta = \left(\frac{J}{\pi x}\right)^2 . \frac{a}{a'} \qquad (A3)$$

b) Blade Element Considerations

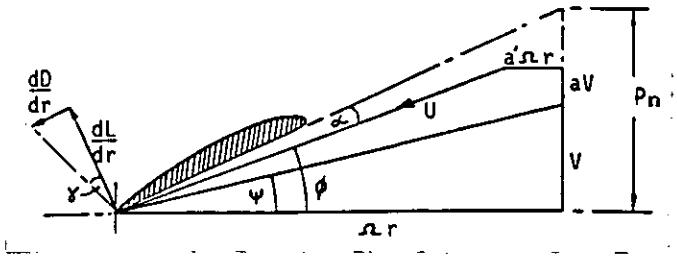

Local lift gradient: $dL/dr = 1/2\rho NcU^2C_L$

Local drag gradient: $dD/dr = 1/2\rho NcU^2C_D$

where C_L and C_D are the section lift and drag coefficients, N is number of blades and c is blade chord.

From the vector diagram:

$$\tan\gamma = C_D/C_L$$

$$\tan(\phi + \alpha) = (P/D)/\pi x$$

$$\tan\gamma = V/\Omega r = J/\pi x$$

$$\tan\phi = V(1 + a)/\Omega r\ (1 - a') = (1 + a)/(1 - a').\tan\psi$$

Resolution of the lift and drag yields the section thrust and torque gradients as:

$$\frac{dK_T}{dx} = \frac{\pi^2}{4}\left(\frac{Nc}{D}\right) C_L x^2(1 - a')^2\sec\phi(1 - \tan\phi.\tan\gamma) \qquad (A4)$$

$$\frac{dK_Q}{dx} = \frac{\pi^2}{8}\left(\frac{Nc}{D}\right) C_L x^3(1 - a')^2\sec\phi(\tan\phi + \tan\gamma) \qquad (A5)$$

and local efficiency as:

$$\eta = \frac{\tan\psi}{\tan(\phi+\gamma)} \qquad (A6)$$

$$\text{or} \qquad \eta = \frac{1 - a'}{1 + a} \cdot \frac{\tan\phi}{\tan(\phi+\gamma)} \tag{A7}$$

where $(1 - a')/(1+a) = \eta_i$ is the ideal efficiency, neglecting friction losses. (A8)

Equating the efficiencies derived from momentum and blade element considerations, equations (A3) and (A7), yields a solution for the axial inflow factor as:

$$a = \frac{1 - \eta_i}{\eta_i + \frac{\tan^2\psi}{\eta}} \tag{A9}$$

Application of equations (A1) to (A9) yields solutions for the thrust and torque gradients (dK_T/dx and dK_Q/dx) and local section efficiency (η). Integration radially across the blade yields total K_T and K_Q values.

Equations (A1) to (A9) are incorporated in the computer program to derive induced velocities and section forces.

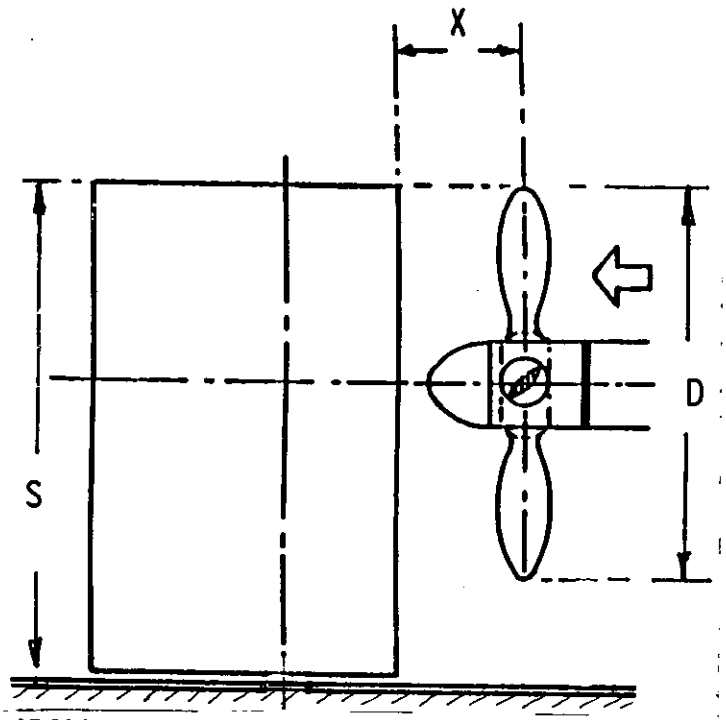

Fig.1 Definitions of Basic Rudder-Propeller Layout

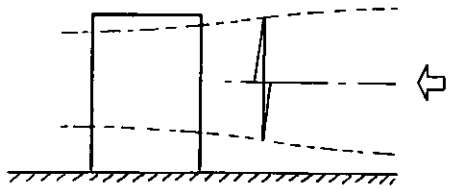

(a) Propeller Race Acceleration and Contraction

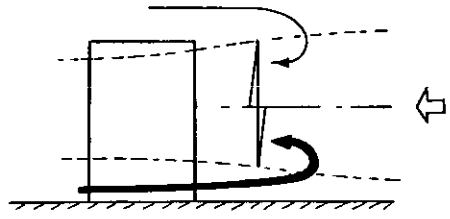

(b) Backflow Adjacent to Hull (or Tunnel Groundboard)

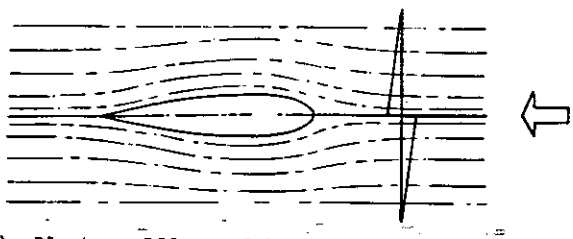

(c) Blockage Effect of Rudder on Propeller

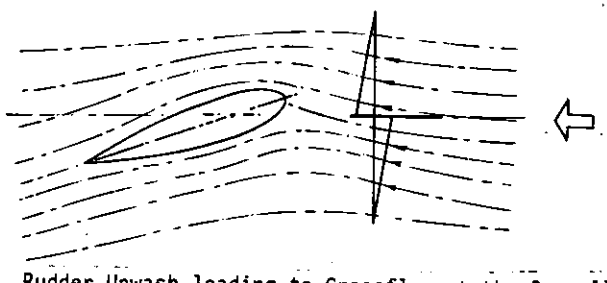

(d) Rudder Upwash leading to Crossflow at the Propeller

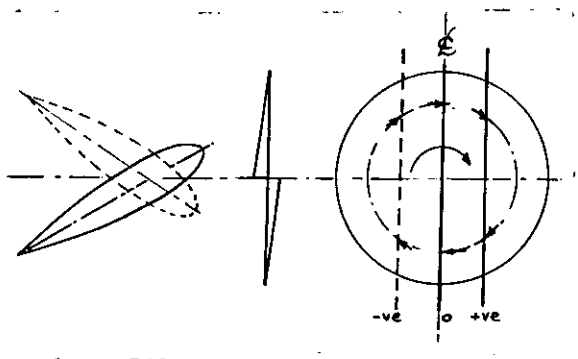

(e) Influence of Rudder Incidence on Interpolation of Induced Velocities

Fig.2 Features of the Physical Fluid Flow

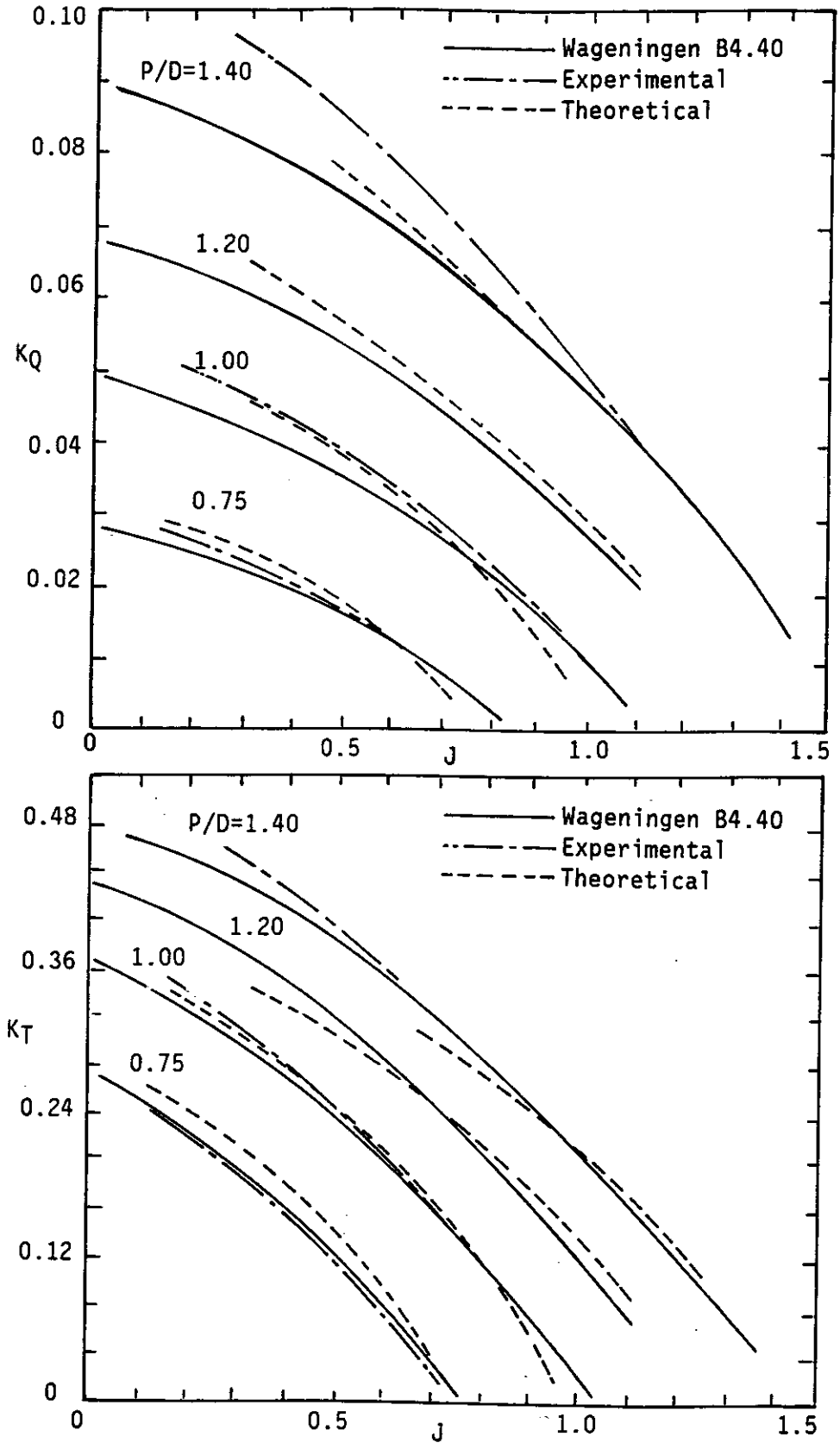

Fig.3 Comparison of Theoretical Results with Experimental Results and values for the Wageningen B4.40 (Ref.12)

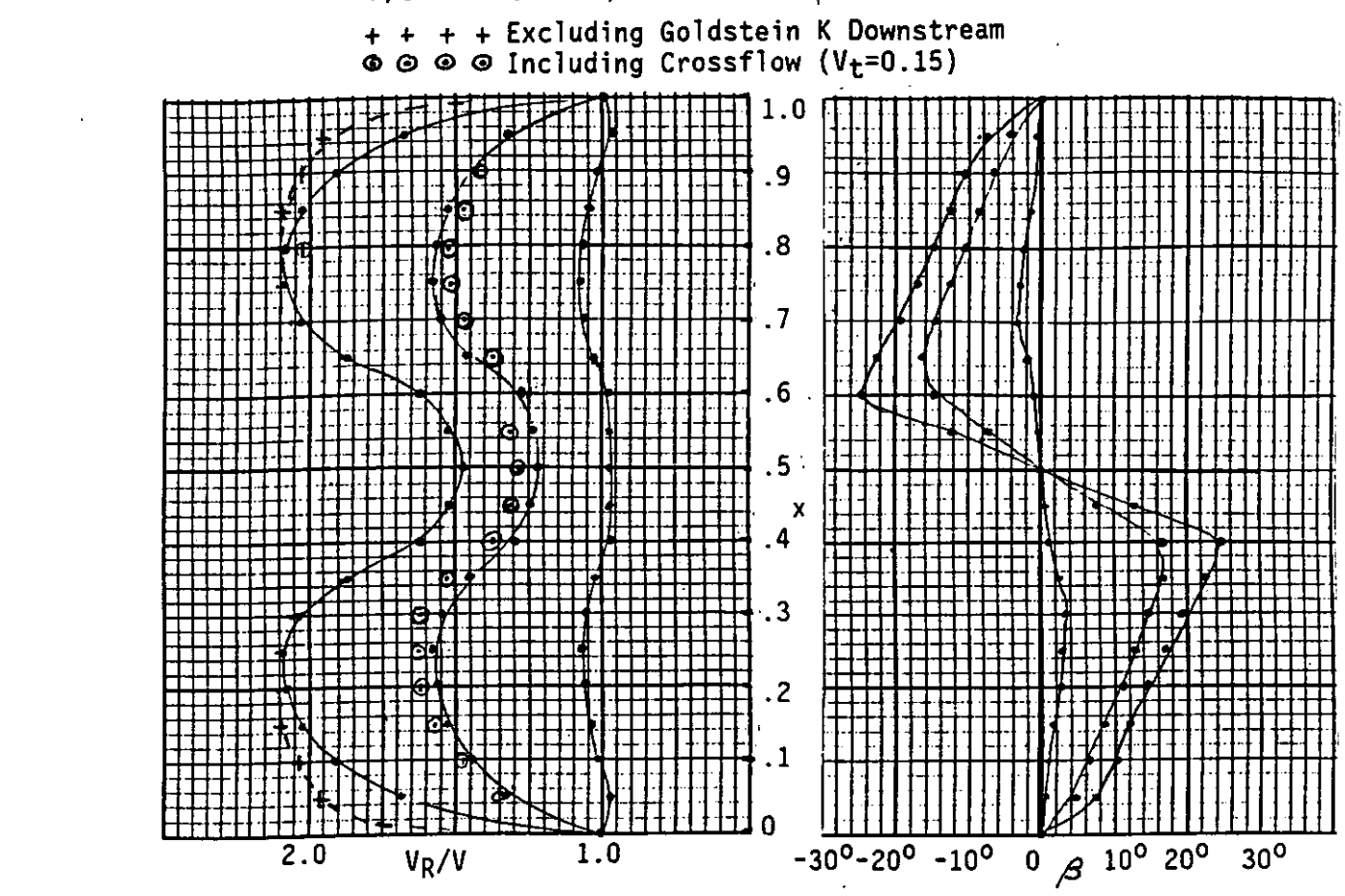

Fig.4 Basic Distributions of Propeller Induced Velocities and Angles (at propeller disc, X/D=0.0)

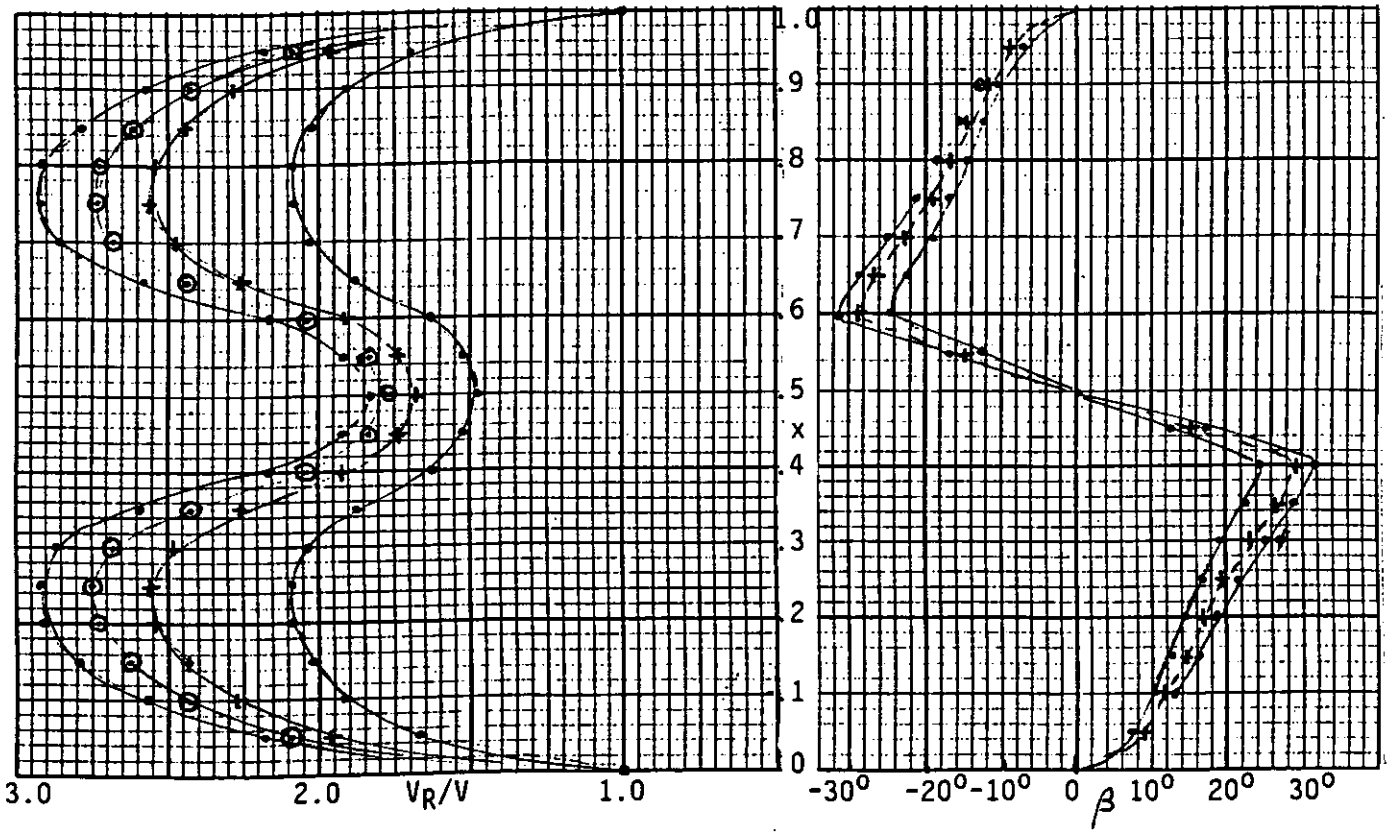

P/D=1.0 X/D=0.0, 0.1, 0.2, 0.4

Fig.5 Influence of Slipstream Acceleration Correction on Propeller Induced Velocities and Angles (J=0.35)

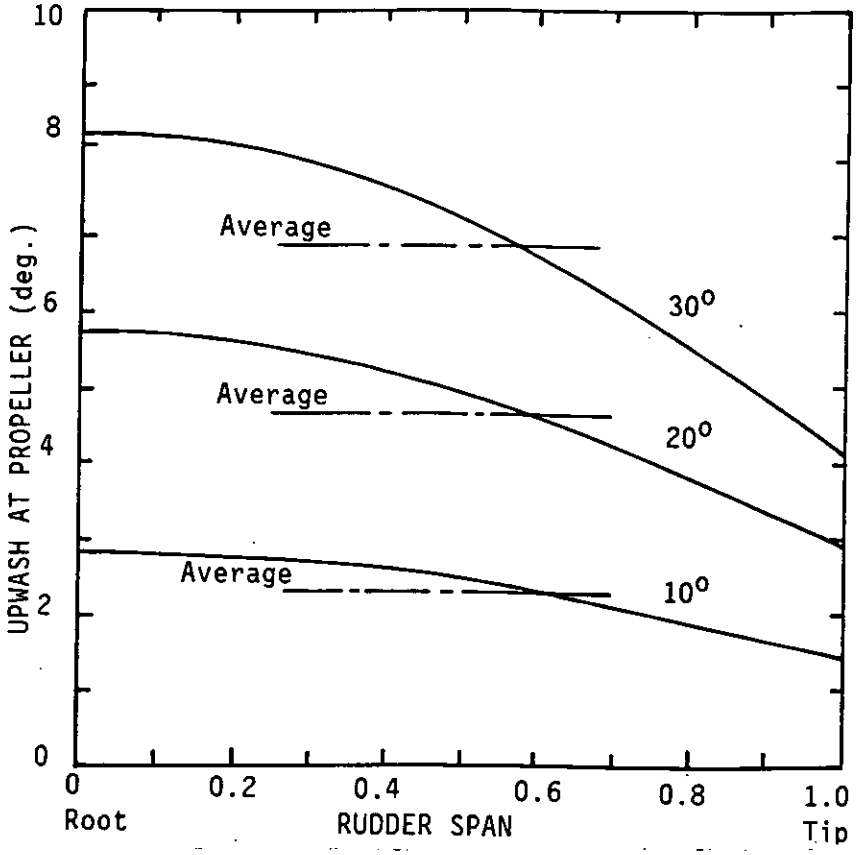

Fig.6 Distribution of Upwash over Rudder Span (X/D=0.39)

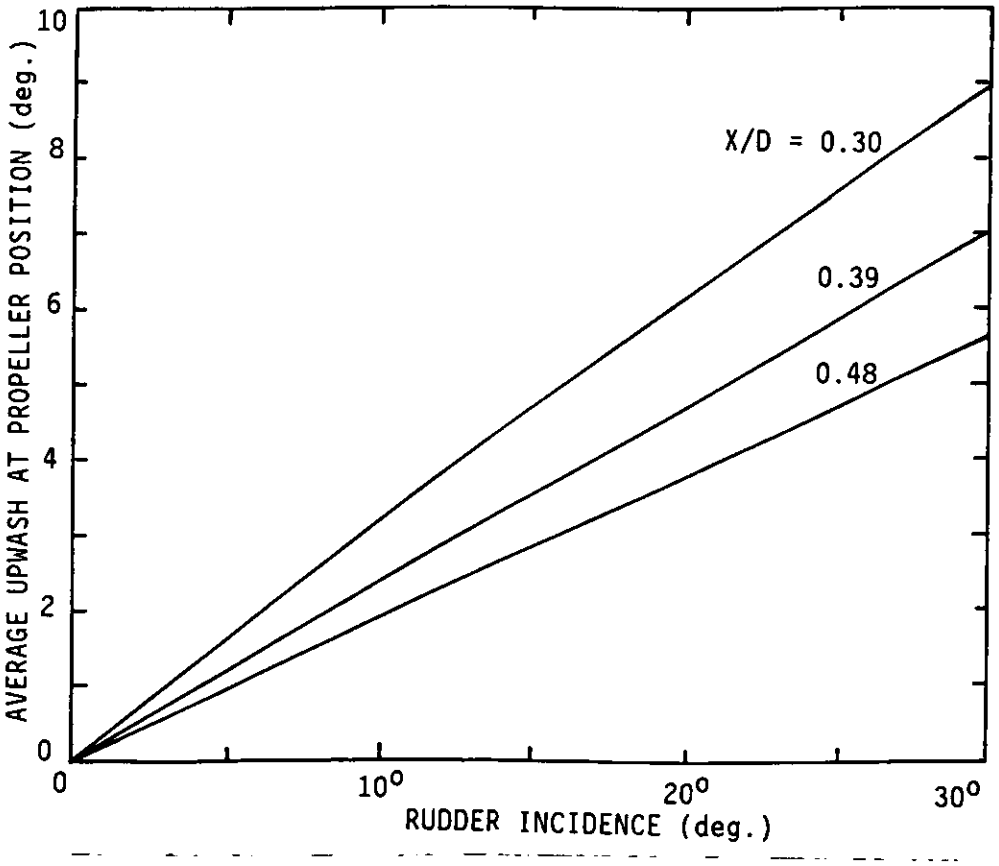

Fig.7 Average Values of Upwash at the Propeller

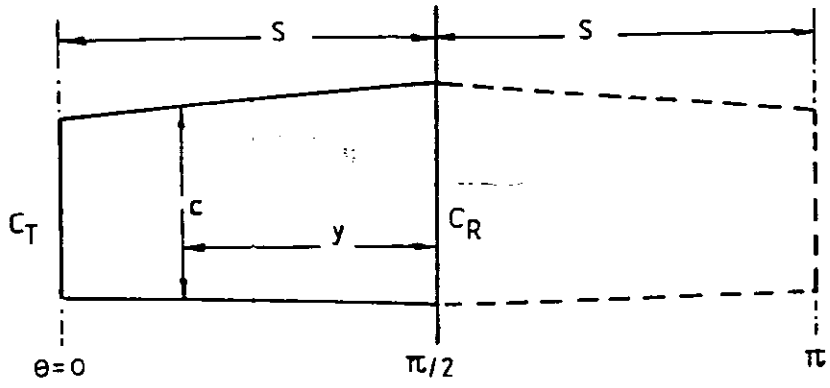

Fig.8 Rudder Geometry used in Analysis

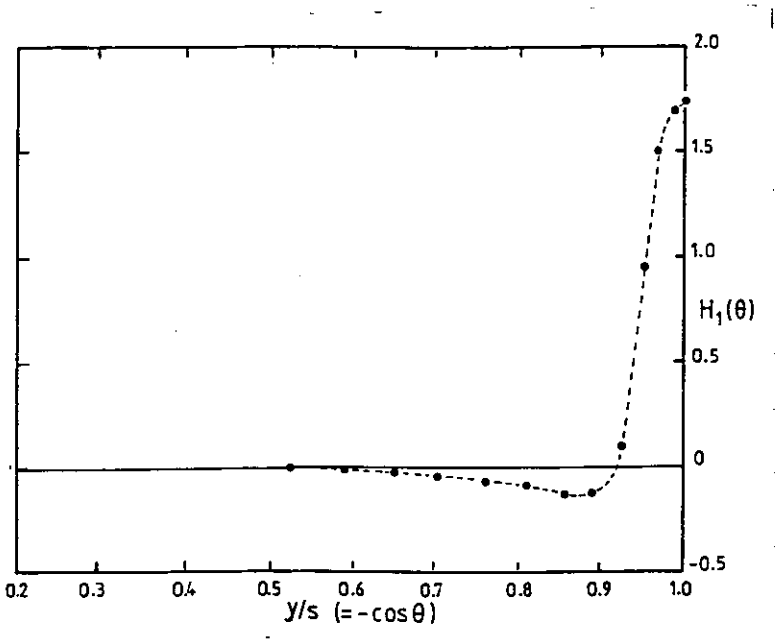

Fig.9 General Form of Function $H_1(\theta)$

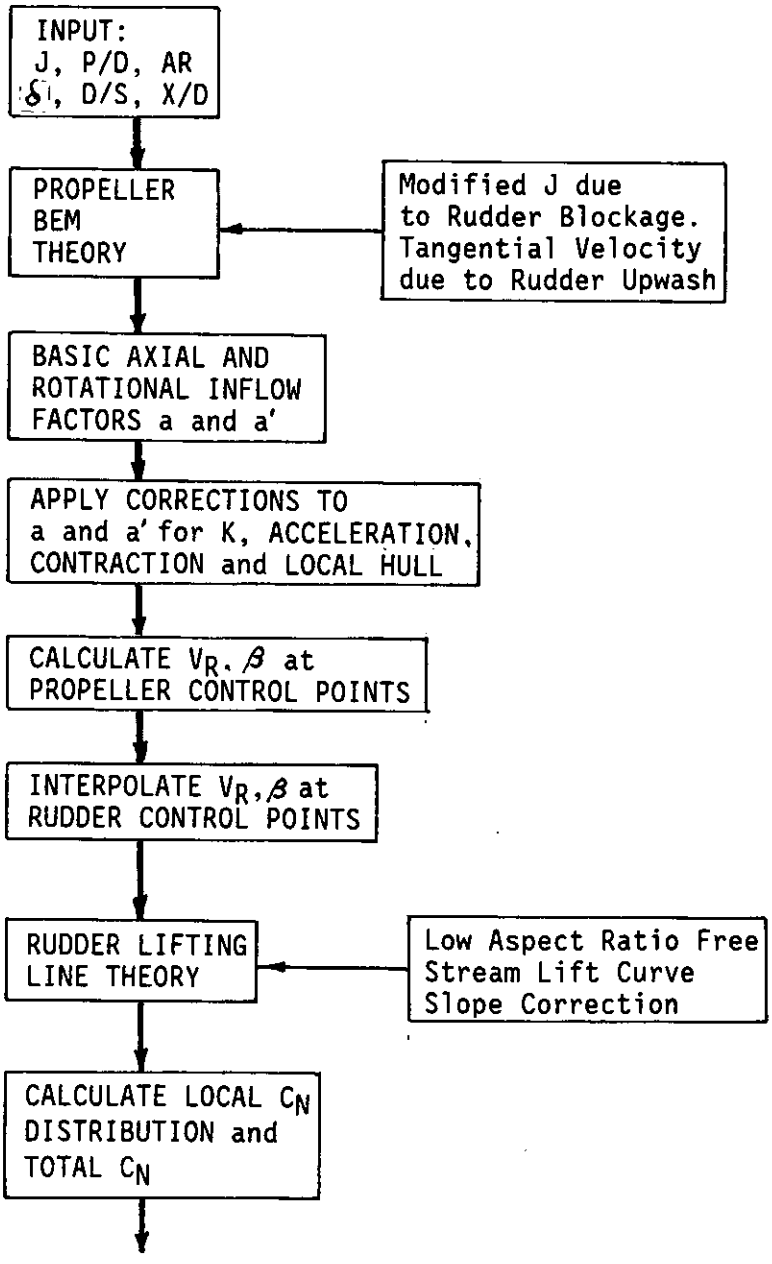

Fig.10 Overall Program Flow Path

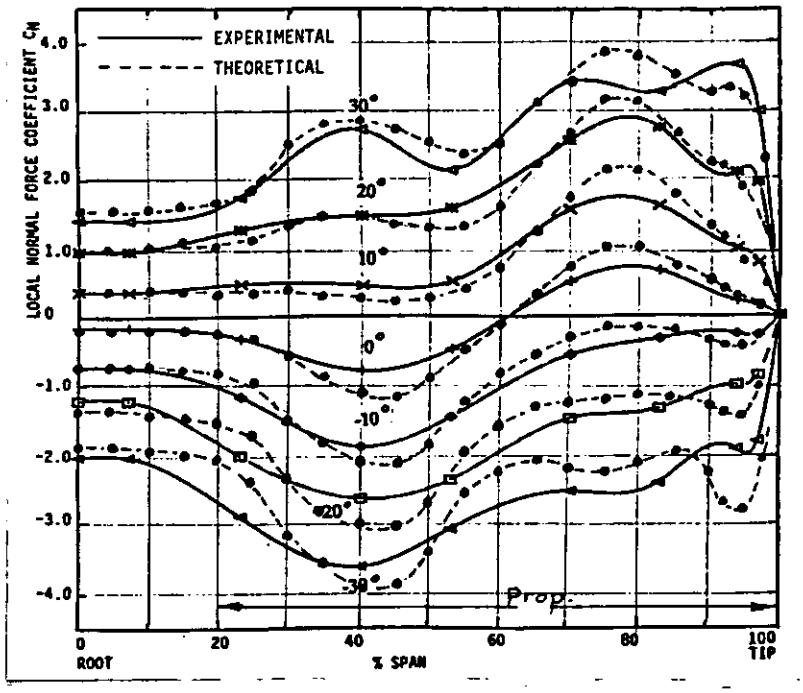

Fig.11a Spanwise Load Distributions, Rudder No.2
X/D=0.39, J=0.51
Comparison of Lifting Line Theoretical
Predictions with Experimental Results

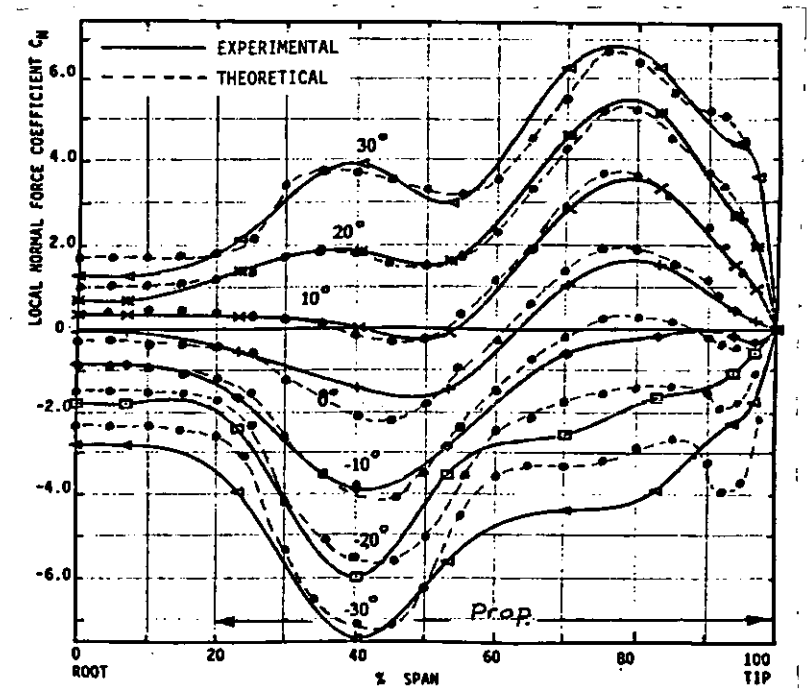

Fig.11b Spanwise Load Distributions, Rudder No.2
X/D=0.39, J=0.35
Comparisons of Lifting Line Theoretical
Predictions with Experimental Results

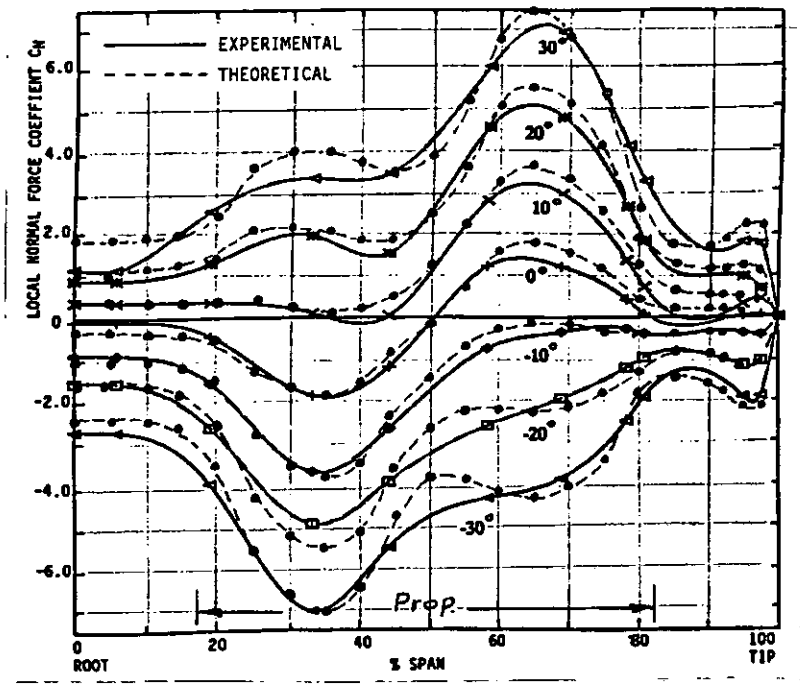

Fig.11c Spanwise Load Distributions, Rudder No.3
X/D=0.39, J=0.35
Comparison of Lifting Line Theoretical
Predictions with Experimental Results

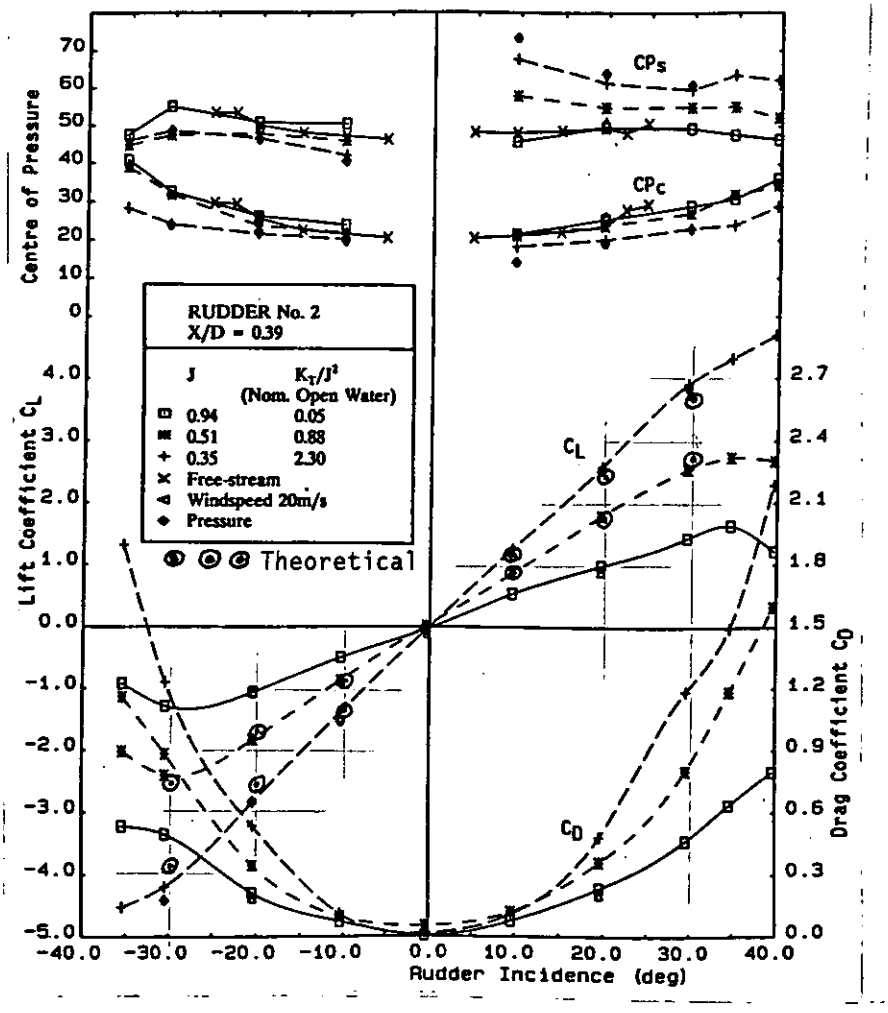

Fig.12 Lift, Drag and Centre of Pressure Characteristics
Comparison of Lifting Line Theoretical Predictions
for Total Lift with Experimental Results

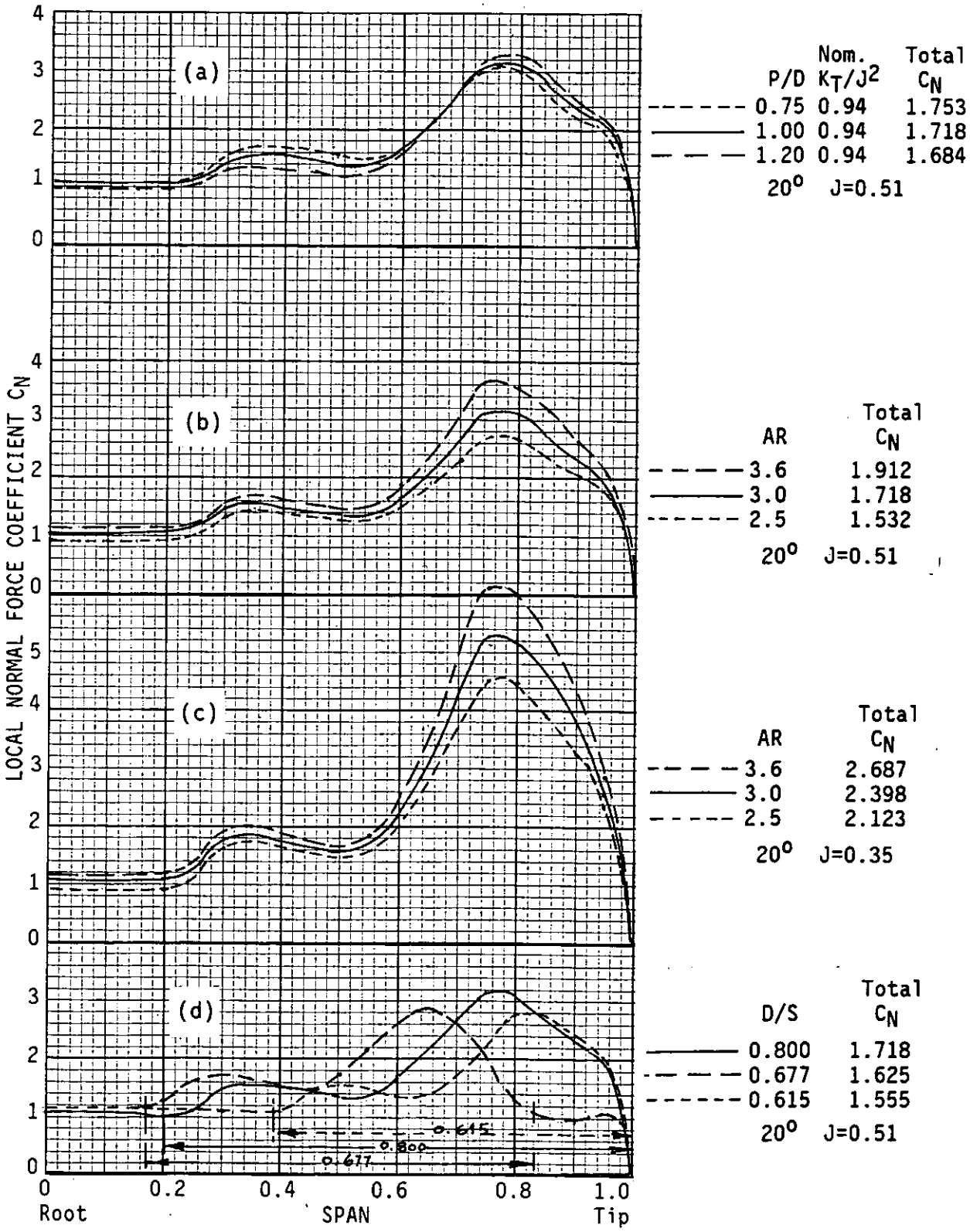

Fig.13 Influence of P/D (for same K_T/J^2), Aspect Ratio and Coverage (D/S) on Spanwise Normal Force Distributions and Total Normal Force